Calorimetric study of white portland cement hydration. Effect of nanosilica and temperature

I.F. Sáez del Bosque[1], S. Martínez-Ramírez [1,2], M.T. Blanco-Varela[1]*

1. Instituto de Ciencias de la Construcción "Eduardo Torroja" (IETCC-CSIC), Consejo Superior de Investigaciones Científicas, 28026, Spain

2. Instituto de Estructura de la Materia (IEM-CSIC), Consejo Superior de Investigaciones Científicas, 28006, Spain

Abstract

Cement manufacture generates environmental problems due, among others, to the greenhouse gases, especially CO_2, emitted in the process. A number of materials have been used as cement additions in recent years to lower such emissions. One of the foremost is nanosilica (nSA), which as a nano-filler and pozzolan enhances the mechanical strength and reduces the porosity of the end product. Portland cement hydration is favoured by both temperature and the presence of nSA.

Calorimetric studies were performed to monitor the early age hydration of white portland cement containing 10 % nSA at 25, 40 and 65 ºC for 24 h. After hydration was detained at trial times defined by the peaks observed on the calorimetric curves, samples cured for those times were characterised by XRD, DTA/TG, and ^{27}Al MAS NMR.

The findings showed that temperature and the addition of nSA induced the same type of alterations in the calorimetric curve: the induction period was shortened and heat flow rose. The calorimetric curve for the nSA-containing pastes cured at 65 ºC exhibited 3 main peaks, one more than the curve for the sample without nSA. Moreover, the ratios between the intensities of the signals varied widely. Nanosilica stabilised ettringite in the samples hydrated at 65 ºC, while that phase was non-existent in the samples without nSA.

Originality

Ettringite decomposes at temperatures of over 40 ºC. The present study shows that adding nSA to white Portland cement stabilises its formation at 65 ºC, a finding that holds great technological promise for the durability of pre-cast concrete.

Keywords: *nanosilica, white portland cement, calorimetry, temperature, ettringite.*

[1] Corresponding author: blancomt@ietcc.csic.es,Tel +34 913020440, Fax +34-3020700

1. Introduction

Modern economic and industrial development has prompted exponential growth in construction and high cement consumption. Heightened social awareness of the adverse environmental effects of the intense extraction of the raw materials required in cement manufacture has been attendant upon those developments. Consequently, cement is now ordinarily replaced in part by other materials to lower CO_2 emissions by reducing the proportion of clinker involved or to improve the properties of the hardened cement. Some of these replacement materials, such as silica fume (SF), fly ash (FA) and blast furnace slag (BFS), included as cement components in European standard EN 197-1 (2011) [1], exhibit pozzolanic or hydraulic properties. Limestone is another type of addition (filler) addressed in the standard. Although it exhibits neither pozzolanicity nor hydraulicity, it hastens the hydration of the silicates present in clinker, particularly if ground to a high specific surface, and interferes in aluminate hydration [2, 3]. Many of the other materials being explored for this use are likewise pozzolanic industrial by-products (rice husk or bagasse ash) (Cordeiro et al., 2012, Lin, 2013). Other nanometric additions such as n-Al_2O_3, n-Fe_2O_3, n-TiO_2, n-Cr_2O_3 and n-SiO_2 have aroused interest in the scientific community for their possible beneficial effect on the hardened end product. These nanoparticles have been shown to hasten the hydration rate of the silicates present in cement, for they act as nucleation sites for C-S-H formation (B. Y. Lee, 2010, Nazari and Riahi, 2011b), and as nano-fillers that reduce porosity (Kontoleontos, 2012, Nazari and Riahi, 2011a).

Amorphous n-SiO_2 (nSA) nanoparticles are insoluble in water, where they form a suspension. A number of studies conducted on how nSA affects cement hydration have revealed that it expedites silicate phase hydration and leads to C-S-H gels with a longer chain length (Sáez del Bosque, 2013a, Sáez del Bosque, 2013b, Shih et al., 2006, Land, 2012). Moreover, while both temperature and the addition of nSA are known to hasten cement hydration (Sáez del Bosque, 2013a), the latter has been shown to affect C_3S hydration more intensely than the former (Sáez del Bosque, 2013a).

Since hydration entails heat release, the effect of temperature and the addition of nSA on that process is a factor well worth researching. In the present study, isothermal conduction calorimetry was used to explore the joint effect of curing temperature and the addition of amorphous nanosilica (nSA) on early age white cement (WPC) hydration. The phases formed were characterised with X-ray diffraction (XRD), differential thermal and thermogravimetric analysis (DTA/TG), ^{27}Al magic angle spinning (MAS) and cross-polarisation magic angle spinning nuclear magnetic resonance (^{27}Al MAS NMR and ^{27}Al CP/MAS NMR).

2. Experimental

The white cement used in this study, classified as BL I 52.5 R in Spanish standard UNE 80305 and nSA used here were characterised in prior studies [10, 14]. White cement pastes were prepared as follows: unadditioned cement with a water/solid (w/s) ratio of 0.425 used as a reference and labelled WPC; cement with 10 % nSA and a w/s of 0.66, labelled WPC+nSA. All pastes were cured at 25, 40 or 65 °C. Given the high specific surface of nSA, different w/s ratios were used to ensure the same workability in all pastes. This was deemed preferable to using plasticisers to reduce the water needed in the additioned pastes, inasmuch as such admixtures alter hydration kinetics.

Calorimetric measurements were recorded at 25, 40 and 65 ºC on a Thermometric TAM Air analyser with water as the external standard. The WPC and WPC-nSA pastes were prepared ex-situ, i.e., outside the calorimeter by mixing the solids with water and stirring vigorously for 3 minutes. The mixes were then placed in the calorimeter vials in less than 5 minutes, after which measurements were recorded for 24 hours. The dry nSA and cement were blended prior to mixing with water. Preliminary analyses conducted with 2.5, 5 and 10 wt% nSA showed that 10 % was the most suitable proportion, for it induced the greatest differences in heat flow relative to the reference (Figure 1).

All the calorimetric curves in this paper are referred to gram of solid (for both pure and mixed samples), not to the total weight of the paste sample. The data reported are based on the mean of various readings per sample.

The reactions taking place at each isothermal conduction calorimetric signal were identified using samples whose hydration was detained with acetone at the times determined by the signals and which were subsequently vacuum dried for 5 h. The characterisation techniques used included differential thermal and thermogravimetric analysis (DTA/TG), X-ray diffraction (XRD) and aluminium nuclear magnetic resonance (^{27}Al MAS NMR).

The ^{27}Al MAS NMR scans were performed on a Bruker Avance-400 (9.4 T) spectrometer operating at a frequency of 104.3 MHz, with a 2-μs π/2 pulse, a 5-s recycle delay and a 10-kHz spinning rate. A total of 128 scans were recorded per sample. An $AlCl_3 \cdot 6H_2O$ solution (δ= 0 ppm relative to TMS) was used as an external standard for the ^{27}Al chemical shifts.

Powder X-ray diffraction (XRD) studies were conducted on a Bruker D8 Advance diffractometer, fitted with a (1.54-Å CuK$\alpha_{1,2}$) copper anode X-ray tube, a Lynxeye detector with a 3-mm antiscatter slit and a 0.5 %, Ni K-beta filter. Readings were taken between 2θ angles of 5-60º.

DTA and TG analyses were run on a TA Instruments SATQ600 thermal analyser, heating the samples from 20 to 1 050 °C at a rate of 10 °C/min in a dynamic N_2 atmosphere (100 ml/min).

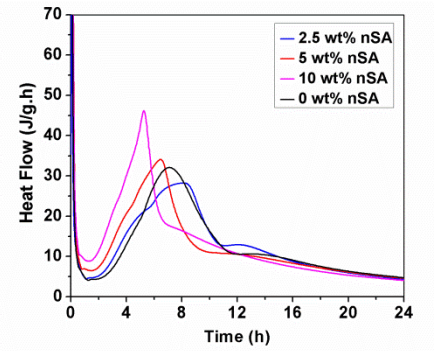

Figure 1. Heat flow for hydrated white cement pastes with 0, 2.5, 5 and 10 % nSA, cured at 25 ºC

3. Results and discussion

All the normalised heat flow curves recorded during nSA-additioned and unadditioned white cement hydration at different curing temperatures (Figure 2) were observed to have two or three more or less well defined peaks. The addition of nSA to the cement induced a substantial change in the curve profile during the first few hours.

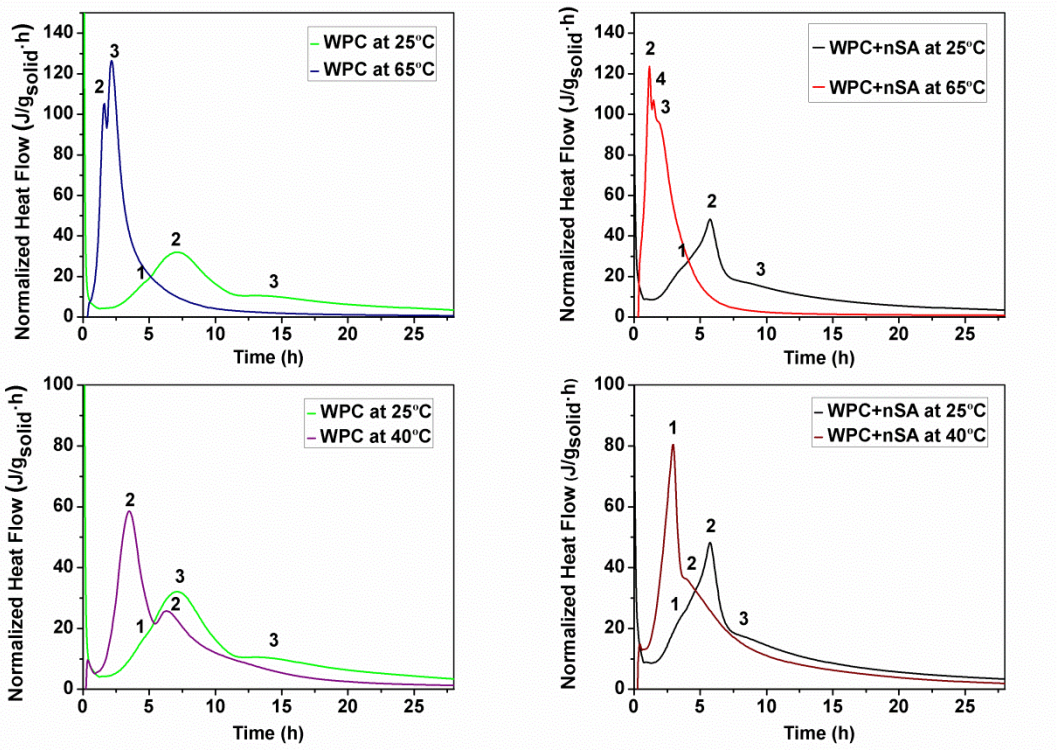

Figure 2. Normalised heat flow for hydrated white cement pastes with and without nSA, cured at different temperatures

The calorimetric curves for the nSA-additioned and unadditioned pastes cured at 25 °C contained three peaks, shown in prior studies [15] using XRD and ^{27}Al MAS NMR to be generated by ettringite formation (peak 1), silicate hydration (peak 2) and ettringite transformation into monosulfoaluminate (peak 3). Moreover, at early hydration ages, the nSA was observed to stabilise ettringite (Ett), retard monosulfate (AFm) formation and fail to stabilise hemicarboaluminate (Hc).

Further to Figure 2, curing temperature induced intense change in the calorimetric curves, the least drastic being recorded for the additioned and unadditioned pastes cured at 40 °C. These pastes exhibited no clear inflection point before the silicate hydration peak (labelled peak 1 and associated essentially with ettringite formation in the pastes cured at 25 °C [15]). This was due to the accelerated hydration of the C_3A + gypsum, which induced ettringite formation, along with hastened silicate hydration. The increase in temperature brought the other two peaks (labelled 2 and 3) forward, intensifying the heat flow (Table 1).

Table 1. Isothermal conduction calorimetry findings for white cement hydration at several curing temperatures, with and without nSA

	25 ºC (Sáez del Bosque I.F., 2013)		40 ºC		65 ºC	
	WPC	WPC + 10 wt% nSA	WPC	WPC + 10 wt% nSA	WPC	WPC + 10 wt% nSA
Peak 1 Time (h)	4.9±0.4	3.75±0.05	-	-	-	-
Peak 1 Heat flow J/g·h)	19±3	33±7	-	-	-	-
Peak 2 Time (h)	7.4±0.4	5.5±0.3	3.7±0.4	2.9	1.61±0.01	1.175±0.007
Peak 2 Heat flow (J/g·h)	33±5	52 ± 3	60±2	80	117±7	128±6
Peak 3 Time (h)	13.1± 0.2	6.9±0.2	6.2±0.2	4.0	2.09±0.06	1.87±0.02
Peak 3 Heat flow (J/g·h)	12 ± 1	18 ± 1	28±4	35	126±2	96.4±0.6
Peak 4 Time (h)	-	-	-	-	-	1.47±0.01
Peak 4 Heat flow (J/g·h)	-	-	-	-	-	108±1

The calorimetric curves for the pastes cured at 65 °C varied substantially from the above. The intensity of the heat flow peaks on the plots for the unadditioned pastes was inverted relative to the curves for the pastes cured at 25 °C: i.e., more heat was released in peak 3 than peak 2. The samples cured at 65 °C revealed the effect of adding nSA: the curve for the additioned paste had three peaks (2, 3 and 4) compared to the two observed in the curve for the unadditioned material. The origins of those peaks, pursuant to the XRD, ^{27}Al MAS NMR and DTA/TG findings for the 65 °C samples whose hydration was detained at the ages at which they appeared, are discussed below.

The XRD study (Figure 3) of the samples of pastes whose hydration was detained at peak 2 (WPC-P2 and WPC+nSA-P2) identified ettringite (Ett) as the sole aluminate phase hydrated. No hemicarboaluminate (Hc) was observed on the XRD pattern. The relative intensity of the diffraction lines for ettringite to a scantly reactive phase such as belite (signals at 9.10º and 39.4º, respectively) was similar in the two pastes (ratios of 0.58 and 0.577, respectively, in the additioned and unadditioned samples). The ratio between the intensities of C_3A and belite (signals at 33.2° and 39.4°, respectively) was smaller in the paste containing nSA, however. The ^{27}Al MAS NMR spectra (Figure 4) confirmed that the sole aluminate phase with octahedrally coordinated Al was ettringite, although the peak formed was somewhat asymmetrical. The cross-polarisation study confirmed the presence of ettringite (signal at 13 ppm), although the identity of the shoulder at a lower ppm value was unclear. It may have been due to monosulfoaluminate, a hemicarboaluminate or merely to noise. Differential thermal analysis (Figure 5) showed water loss at 86 °C from ettringite dehydration, unbound water and the water in C-S-H gel. No water loss at or around 150 °C, which might have denoted the presence of monosulfate or Hc, was observed. The inference is that the additional signal observed on the ^{27}Al CP/MAS NMR spectrum was due to noise.

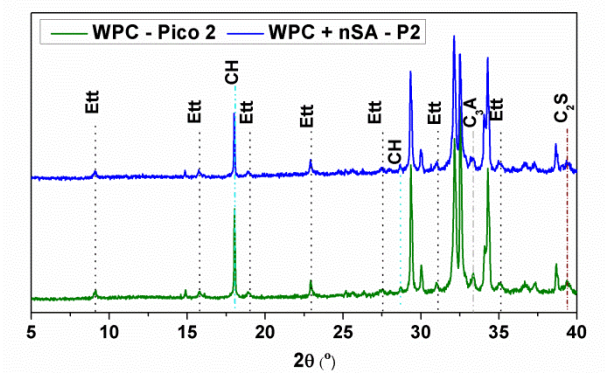

Figure 3. XRD patterns for WPC+nSA and WPC pastes cured at 65 °C for the times defined by calorimetric curve peak 2

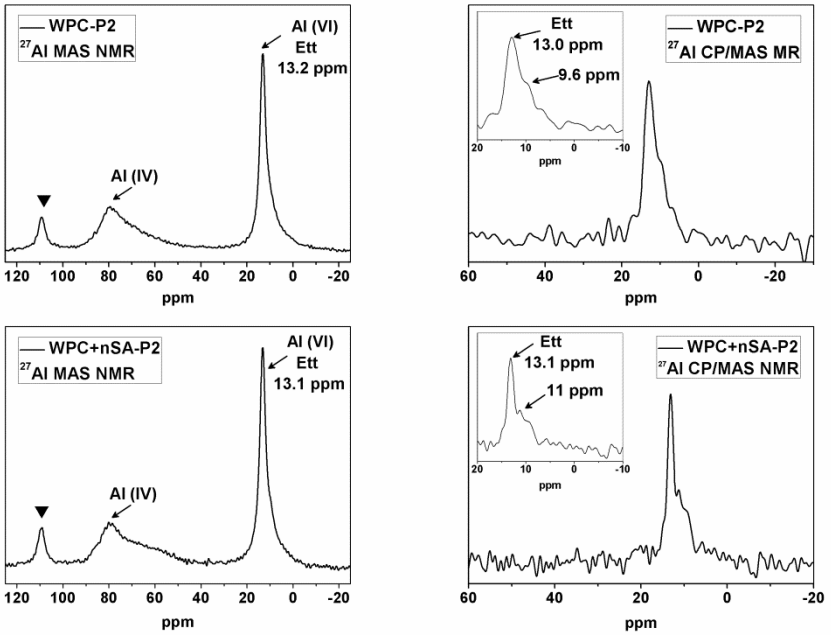

Figure 4. ^{27}Al MAS NMR and ^{27}Al CP/MAS NMR spectra for WPC and WPC+nSA pastes cured at 65 °C for the times defined by calorimetric curve peak 2 (▼= spinning sideband)

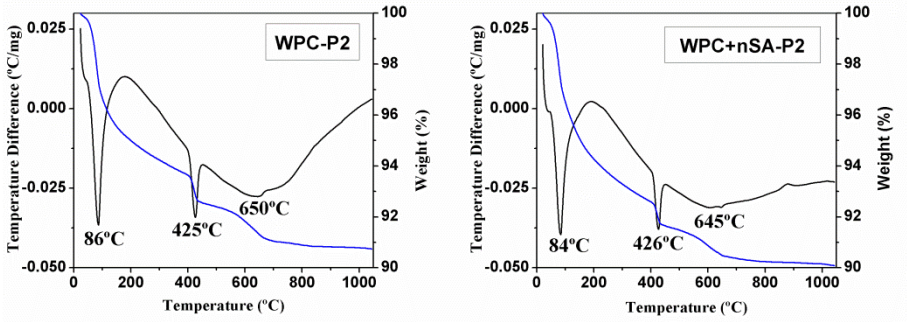

Figure 5. Differential thermal and thermogravimetric (DTA/TG) analysis of pastes WPC and WPC+nSA cured at 65 °C for the times defined by calorimetric curve peak 2

The TG data showed that the weight loss associated with portlandite dehydroxylation at peak 2 was greater in the unadditioned than in the additioned paste (Table 2). This may be an indication that the nSA reacted with the portlandite to generate additional C-S-H gel from a very early stage. When analysing these data, account must be taken of the fact that the sample bearing nSA contained 10 % less alite and C_3A and consequently less portlandite and even less ettringite. The curing age, which was shorter in the nSA-bearing sample, must also be taken into consideration, for it would redound to a lower degree of hydration and therefore a smaller proportion of portlandite. Nonetheless, further to the TG data, 15 % more chemically combined water was released by C-S-H gel and ettringite dehydration in the WPC+nSA-P2 than in the WPC-P2 sample, denoting a greater amount of C-S-H gel in the former, assuming the same amount of ettringite. Since paste WPC+nSA-P2 had more C-S-H gel and less portlandite than paste WPC-P2, the nSA must have reacted with the portlandite to form C-S-H gel, in turn stimulating alite hydration.

According to the literature (Taylor, 1997), the first intense peak observed on the calorimetric curve for a hydrated cement paste is generated by silicate hydration, given suitable proportions of C_3A and gypsum. The respective reaction kinetics are governed by C-S-H gel nucleation and increased density, as well as portlandite precipitation. Since in the additioned samples, however, the nSA had already begun to react at that hydration time, the peak must have also been generated by its pozzolanic reaction.

Thomas et al. (Thomas et al., 2009) showed that C-S-H gel added during C_3S hydration at ambient temperature acted as a seed for the formation of more silicate hydration-induced gel as a result of the new nucleation sites. That in turn raised the rate and degree of C_3S dissolution (Thomas et al., 2009, Alizadeh, 2009). According to Alizadeh et al. (Alizadeh, 2009), the intensity of the acceleration due to the addition of C-S-H gel depends on the amount added and its chemical composition (Alizadeh, 2009). The C-S-H from the nSA pozzolanic reaction in sample WPC+nSA-P2 might, then, have acted as a seed, hastening silicate hydration. That would also explain the earlier appearance of peak P2 and the greater heat flow in paste

WPC+nSA than in paste WPC. Lastly, during calorimetric curve peak 2 formation, the addition of nSA induced greater heat flow at all curing temperatures (Table 1) due to the aforementioned hastening effect.

Table 2.Weight loss (P) and percentage by weight (W) of the phases forming at isothermal conduction calorimetry peak 2 during the hydration of WPC and WPC+nSA cured at 65 °C

	WPC – peak 2	WPC+nSA – peak 2
PCH (%)	1.39	1.28
WCH (%)	5.71	5.25
$PCaCO_3$ (%)	1.39	1.18
$WCaCO_3$ (%)	3.17	2.69
P total	9.21	9.86
P H_2O C-S-H + ettringite	6.43	7.40

PCH = portlandite decomposition-induced H_2O loss; $PCaCO_3$ = loss of CO_2 due to descarbonation of calcium carbonate; WCH = portlandite in wt%; $WCaCO_3$ = calcium carbonate in wt%

In calorimetric curves for ordinary portland cement paste cured under standard conditions (20-25 °C), the peak appearing at the longest hydration time and with the lowest heat flow has traditionally been associated with the transformation of ettringite into monosulfoaluminate (AFm) (Taylor, 1997). Nonetheless, some authors associate it with new ettringite forming as a result of the reaction between C_3A and a further source of sulfate ions, namely the species adsorbed onto the C-S-H gel (secondary ettringite formation) (Quennoz, 2012, Quennoz, 2013, Bullard et al., 2011). Prior studies (Sáez del Bosque I.F., 2013) on WPC hydration at 25 °C attributed the aforementioned peak to the transformation of ettringite into monosulfoaluminate, rather than to secondary ettringite formation.

The XRD study (Figure 6) of the pastes cured at 65 °C whose hydration was detained at peak 3 (WPC-P3 and WPC+nSA-P3) revealed that ettringite did not transform into monosulfoaluminate, but rather, together with the ettringite identified in the preceding peaks, formed calcium hemicarboaluminate (Hc) as the hydrated aluminate phase. Furthermore, the relative ratio between the intensities of ettringite (2θ=9.10º) and belite (2θ=39.4º) was higher in the paste with than in the sample without nSA, denoting a wider field of stability for ettringite in its presence than in its absence. That behaviour differed clearly from what was observed in peak 2, in which the ratio was similar in the additioned and unadditioned pastes. Moreover, C_3A hydration continued and only the diffractogram for the unadditioned paste contained a small signal attributable to the anhydrous phase of the aluminate. That phase would still be available to react with ettringite to form calcium monosulfoaluminate hydrate at longer hydration times. The C_3A (2θ=33.24º)/belite (2θ=39.4º) intensity ratio was lower than in the pattern for the calorimetric curve peak 2 material.

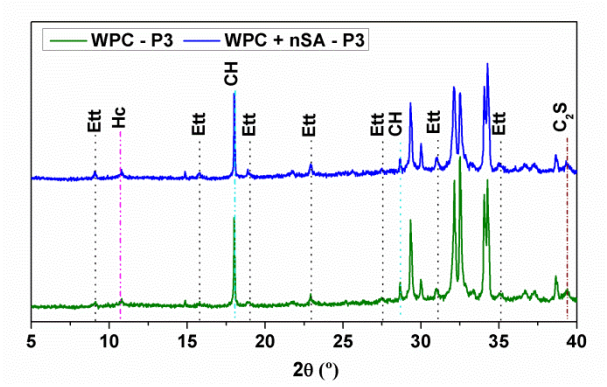

Figure 6. XRD patterns for WPC+nSA and WPC cured at 65 °C for the times defined by calorimetric curve peak 3

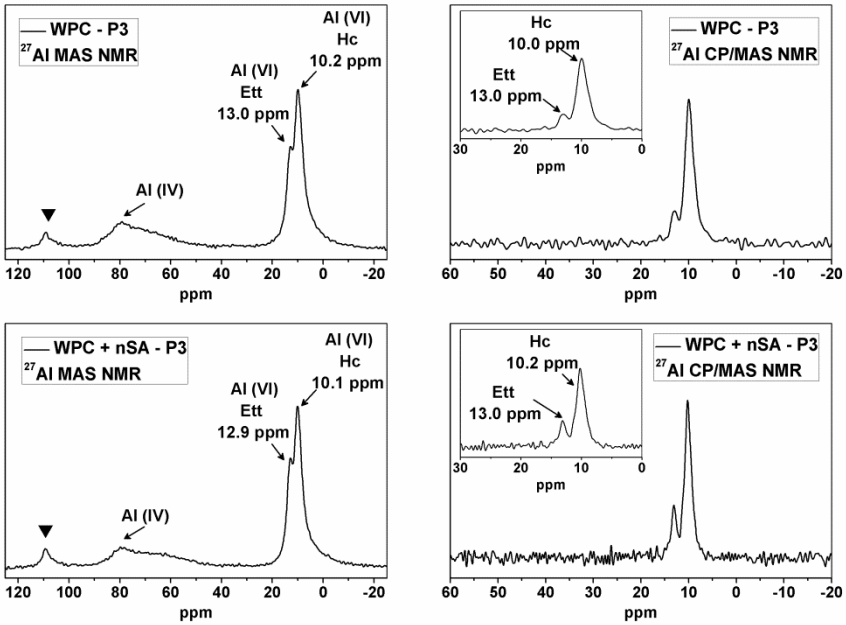

Figure 7. ^{27}Al MAS NMR and ^{27}Al CP/MAS NMR spectra for WPC and WPC+nSA pastes cured at 65 °C for the times defined by calorimetric curve peak 3 (▼=spinning sideband)

The ^{27}Al MAS NMR spectra for both pastes cured at 65 °C whose hydration was detained at calorimetric curve peak 3 (WPC-P3 and WPC+nSA-P3) exhibited signals characteristic of ettringite and calcium hemicarboaluminate, although in different proportions. The paste containing nSA had an Hc/Ett intensity ratio of 1.4, whereas in paste WPC the ratio was 1.5, denoting greater ettringite stability in the former. The ^{27}Al CP/MAS NMR spectra contained two well-defined peaks, one each for Ett and Hc, as observed in the MAS trial, corroborating the XRD findings.

Thermogravimetric analysis (Table 3) showed that silicate hydration continued with curing time: both pastes exhibited greater loss due to portlandite dehydroxylation than the pastes in which hydration was detained at the peak 2 time. As in that case, the paste containing nSA had a smaller percentage of portlandite. In addition, its C-S-H + ettringite water loss was 21 % higher than in the unadditioned paste, again suggesting the existence of a pozzolanic reaction at the early age studied.

Table 3. Weight loss (P) and percentage by weight (W) of the phases forming at isothermal conduction calorimetry peak 3 during the hydration of WPC and WPC+nSA cured at 65 °C

	WPC – peak 3	WPC+nSA – peak 3
PCH (%)	2.37	2.12
WCH (%)	9.72	9.13
$PCaCO_3$ (%)	1.72	1.51
$WCaCO_3$ (%)	3.91	3.43
Ptotal	11.64	12.83
P H_2O from C-S-H and ettringite	7.55	9.20

PCH = portlandite decomposition-induced H_2O loss; $PCaCO_3$ = loss of CO_2; WCH = portlandite in wt%; $WCaCO_3$ = calcium carbonate in wt%

Lastly, peak 4 on the calorimetric curve (in-between peaks 2 and 3) was only observed on the paste containing nSA and cured at 65 °C (WPC + nSA-P4). It would initially be associated with silicate hydration. Ettringite (Ett) and hemicarboaluminate (Hc) were identified on the XRD patterns as the hydrated aluminate phases. The ($C_3A(2\theta=33.24^o)$/belite($2\theta=39.4^o$) intensity ratio was lower than in paste WPC+nSA-P2, evidence of highly exothermal C_3A dissolution and a higher Ett/belite ratio.

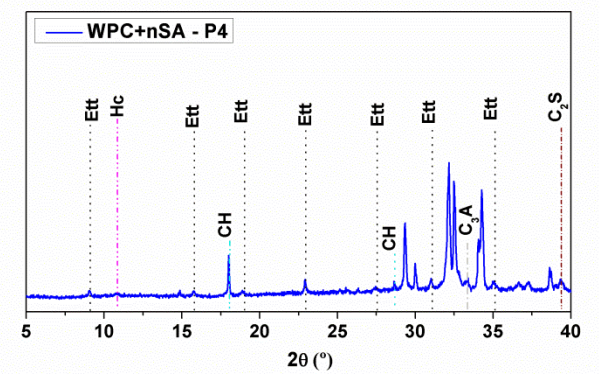

Figure 8. XRD patterns for WPC+nSA and WPC cured at 65 °C for the times defined by calorimetric curve peak 4

The ^{27}Al MAS NMR spectra had two signals in the octahedral aluminium range, at around 13.0 and 9.95 ppm. The first was attributed to ettringite, while the second, located between the ppm values for calcium monosulfoaluminate and calcium hemicarboaluminate, could not be clearly associated with either of these compounds. Three peaks were identified on the ^{27}Al CP/MAS NMR spectra: ettringite at 13.0 ppm and two others, one at 10.2 ppm, characteristic of Hc and the other at 9.65 ppm, associated with AFm. This third phase was fairly amorphous as it was not detected with XRD.

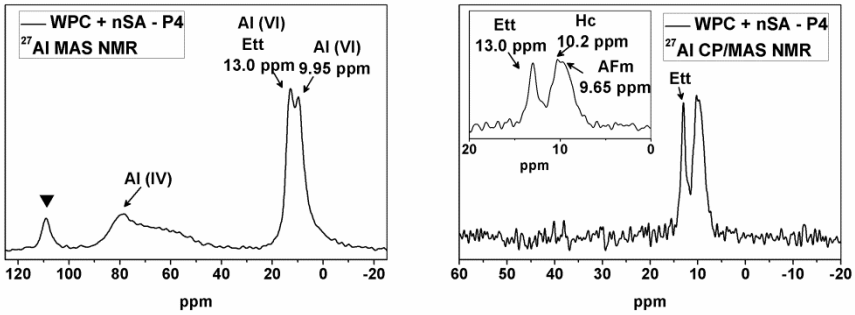

Figure 9. ^{27}Al MAS NMR and ^{27}Al CP/MAS NMR spectra for WPC and WPC+nSA pastes cured at 65 °C for the times defined by calorimetric curve peak 4 (▼=spinning sideband)

The hydration reaction in the pastes cured at 65 °C was also monitored with XRD at t=24 h (Figure 10), at which time no significant difference was observed in the heat flow in the calorimetric curves for the additioned and unadditioned pastes (0.92 J/g·h and 0.85 Jg·h, respectively (Figure 1)). The diffractograms showed that in the nSA-containing pastes, the C_3A phase disappeared entirely and the intensity of the diffraction line for Ett was slightly less intense than on the peak 3 diffractogram. The small wide shoulder at around 10º observed in the XRD papttern of WPC+nSA at 24h might be associated with AFm. Nor was C_3A identified on the XRD patterns for the unadditioned pastes cured at 65 °C. Furthermore, the Hc phase, which appeared at a shorter hydration time (peak 3 on the calorimetric curve), was shown to be the sole stable aluminate hydrate at 24 h.

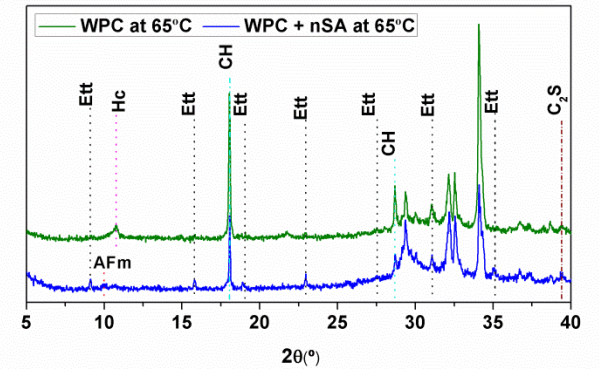

Figure 10. Diffractograms for 24-hour additioned (WPC+nSA) and unadditioned (WPC) pastes cured at 65 °C

The ^{27}Al MAS NMR spectrum for white cement paste containing nSA (in Figure 11) exhibited several signals in the octahedral Al^{3+} range: a very highly resolved peak at around 9.53 ppm, another at around 4.4 ppm and a poorly resolved shoulder at around 12.9 ppm. These peaks were clearly resolved in the ^{27}Al

CP/MAS NMR spectrum, where two signals were observed, one at around 13.1 ppm generated by ettringite and the other at 9.7 ppm associated with monosulfate. In contrast, the ^{27}Al MAS NMR and ^{27}Al CP/MAS NMR spectra for the unadditioned white cement paste contained just one signal at around 10.2 ppm attributed to hemicarboaluminate, confirming the XRD results.

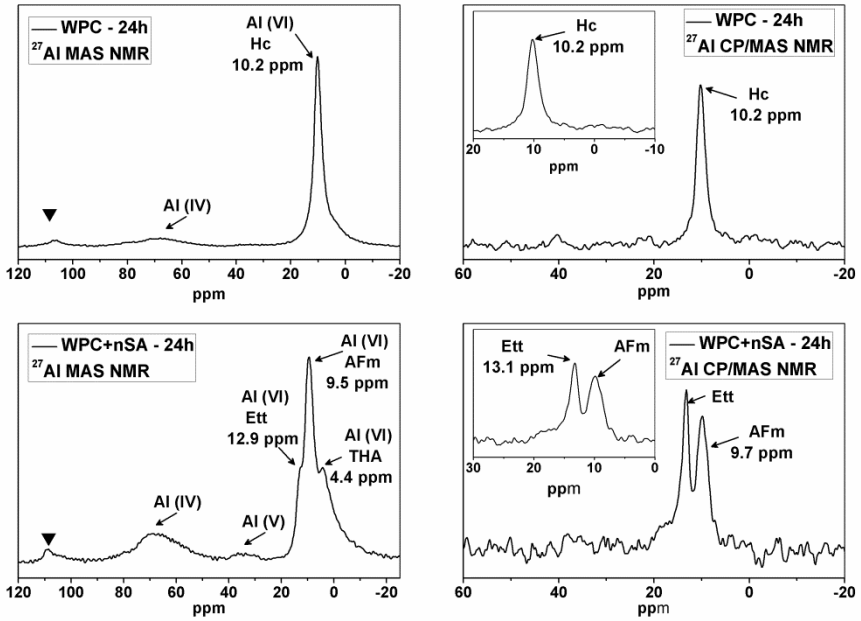

Figure 11. ^{27}Al MAS NMR and ^{27}Al CP/MAS NMR spectra for 24-hour additioned and unadditioned pastes cured at 65 °C (▼ =spinning sideband)

In the 24-hour pastes, the percentage by weight of portlandite (Table 4) was much greater in the sample containing nSA than in the material without the addition due to the pozzolanic reaction taking place after the first 2 h of hydration.

Table 4. Weight loss (P) and percentage by weight (W) of the phases forming in 24-h WPC and WPC+nSA cured at 65 °C (Sáez del Bosque, I.F., 2013b)

	WPC – 24h	WPC+nSA – 24h
PCH (%)	5.12	2.80
WCH (%)	21.05	11.51
$PCaCO_3$ (%)	2.61	3.71
$WCaCO_3$ (%)	4.39	8.43

PCH = portlandite decomposition-induced H_2O loss; $PCaCO_3$ = loss due to calcium carbonate decarbonation; WCH = portlandite in wt%; $WCaCO_3$ = calcium carbonate in wt%

4. Conclusions

The conclusions that may be drawn about the effect of curing temperature and the addition of nSA on the stability of white cement hydration products are listed below.

- Curing temperature hastens the hydration of the silicates and aluminates present in the cement, generating greater heat flow rates at earlier curing times. The addition of nSA has a similar effect. Nonetheless, at the same curing temperature, the additioned pastes generate a higher heat flow due to the nSA-induced acceleration of silicate hydration.
- Amorphous, high specific surface nSA reacts with portlandite from the very first hours of hydration in the paste cured at 65 °C.
- During the first 3-5 h of hydration, the inclusion of nSA induces no change in aluminate phase stability. Ettringite is the sole aluminate hydrate, although after approximately 2 hours of hydration, ettringite is more stable in the additioned than the unadditioned paste cured at 65 °C.
- In young (24-hour) pastes cured at high (65 °C) temperatures, the addition of nSA stabilises ettringite. In unadditioned pastes no ettringite exists due to its instability at such temperatures, the only aluminate hydrate formed being calcium hemicarboaluminate.

Acknowledgements

This research was funded by the Spanish Ministry of Education and Science (MAT2006-11705 and CONSOLIDER CSD2007-00058) and the Regional Government of Madrid (Geomaterials Programme, S2009/MAT-1629). Research fellowship BES-2007-16686 is gratefully acknowledged.

References

Alizadeh, R., Raki, L., Makar, J. M., Beaudoin, J. J., Moudrakovski, I. 2009. Hydration of tricalcium silicate in the presence of synthetic calcium-silicate-hydrate. *Journal of Materials Chemistry,* 19**,** 7937-7946.

B. Y. Lee, K. E. K. 2010. Influence of TiO_2 Nanoparticles on Early C_3S Hydration. *Journal of the American Ceramic Society,* 93**,** 3399-3405.

Bullard, J. W., Jennings, H. M., Livingston, R. A., Nonat, A., Scherer, G. W., Schweitzer, J. S., Scrivener, K. L. & Thomas, J. J. 2011. Mechanisms of cement hydration. *Cement and Concrete Research,* 41**,** 1208-1223.

Cordeiro, G. C., Toledo Filho, R. D., Tavares, L. M. & Fairbairn, E. M. R. 2012. Experimental characterization of binary and ternary blended-cement concretes containing ultrafine residual rice husk and sugar cane bagasse ashes. *Construction and Building Materials,* 29**,** 641-646.

Kontoleontos, F., Tsakiridis, P.E., Marinos, A., Kaoidas, V., Katsioti, M. 2012. Influence of colloidal nanosilica on ultrafine cement hydration: Physicolchemical and microstructural characterization. *Construction and Building Materials,* 35**,** 347-360.

Land, G., Stephan, D. 2012. "The influence of nano-silica on the hydration of ordinary Portland cement". *Journal of Materials Sciencie,* 47**,** 1011-1017.

Lin, L.-K., Wu, W-S., Lee, H. 2013. Value analysis and properties investigation of high performance rice husk ash concrete. *Advanced Materials Research,* 773**,** 293-297.

Nazari, A. & Riahi, S. 2011a. Improvement compressive strength of concrete in different curing media by Al2O3 nanoparticles. *Materials Science and Engineering: A,* 528**,** 1183-1191.

Nazari, A. & Riahi, S. 2011b. The effects of Cr2O3 nanoparticles on strength assessments and water permeability of concrete in different curing media. *Materials Science and Engineering: A,* 528**,** 1173-1182.

Quennoz, A., Scrivener, K.L. 2012. "Hydration of C_3A-gypsum systems". *Cement and Concrete Research,* ***42*****,** 1032-1041.

Quennoz, A., Scrivever K.L. 2013. Interactions between alite and C3A-gypsum hydrations in model cements. *Cement and Concrete Research,* 44**,** 46-54.

Shih, J.-Y., Chang, T.-P. & Hsiao, T.-C. 2006. Effect of nanosilica on characterization of Portland cement composite. *Materials Science and Engineering: A,* 424**,** 266-274.

Sáez Del Bosque I.F., M.-P. M., Martinez-Ramirez, S., Blanco Varela, M.T. 2013. Effect of nanosilica addition on white cement hydration at 25ºC. *International Congress on Materials and Structural Stability (CMSS).* Rabat, Moroco.

Sáez Del Bosque, I. F., Martín-Pastor, M., Martínez-Ramírez, S., Blanco-Varela, M.T 2013a. Effect of temperature on C_3S and C_3S + nanosilica hydration and C-S-H gel structure. *Journal of the American Ceramic Society*, 96**,** 957-965.

Sáez Del Bosque, I. F., Martínez-Ramírez, S., Blanco-Varela, M.T 2013b. Combined Effect of Amorphous Nanosilica and Temperature on White Portland Cement Hydration *Industrial & Engineering Chemistry Research***,** 11866-1187.

TAYLOR, H. F. W. 1997. *"Cement Chemistry",* London, U.K.

Thomas, J. J., Jennings, H. M. & Chen, J. J. 2009. Influence of Nucleation Seeding on the Hydration Mechanisms of Tricalcium Silicate and Cement. *Journal of Physical Chemistry C,* 113**,** 4327-4334.